Progress In Electromagnetics Research B, Vol. 74, 155–171, 2017

A Novel DNG Medium Formed by Ferromagnetic Microwire Grid

Tarun Kumar[1, *] and Natarajan Kalyanasundaram[2]

Abstract—Effective permittivity and permeability of a medium consisting of an infinite number of ferromagnetic microwires are evaluated in this paper. Analysis is carried out with the help of local and average fields inside a unit cell. In the literature, effective permittivity of the microwire grid is obtained by assuming the grid as an impedance loaded surface. The analysis is applicable only for the case of TM_z polarized normally incident wave. Proposed analysis enable us to evaluate all the three diagonal components of effective permittivity and permeability for arbitrarily incident uniform plane wave having arbitrary polarization angle. Numerical results are obtained through MATLAB, and a comparison is done with the results available in the literature for validation. Numerical results have shown a DNG like behaviour of the medium for a TM_z polarized incident wave.

1. INTRODUCTION

The decades of the 1990s and 2000s had renewed interest and fervor in the field of electromagnetics, due to the development of metamaterials [1–6]. The word 'Metamaterial' was initially presented in University of Texas at Austin by Rodger M. Walser, in 1999 [5]. The first attempt to introduce the concept of artificial materials in microwave engineering was made by Jagadis Chander Bose in 1898. The first microwave experiment on twisted jute structures was conducted by him which is artificial chiral material [7]. In 1914, Lindell et al. [1] studied an artificial chiral medium formed by an ensemble of small wire helices. In 1948, Kock [8] put forward the concept of light weight lenses at microwave frequencies utilizing artificial dielectric. In 1967, a Russian physicist Viktor Veselago put his revolutionary idea about the possibility of substances with $\epsilon < 0$ and $\mu < 0$ [9]. It has been reported by many researchers that the dispersion characteristics of the "rodded" dielectric medium, or "conducting strip medium" has shown the characteristics like a plasma [10–12]. In 1996, Pendry et al. [2] proposed the wire medium which consist of metallic wires arranged like a mesh. This medium acts like an artificial electric plasma which possesses negative permittivity. In 1999, Smith et al., proposed the artificial magnetic plasma having negative permeability [3]. By applying the approach suggested by Pendry et al. [2] on a grid consisting of ferromagnetic microwires instead of metallic wires, it is possible to attain Double Negative (DNG) behavior with only single type of element without using separate inclusions for negative permittivity and permittivity. Ferrites are known to have negative permeability in certain frequency range, subjected to the condition of ferromagnetic resonance (FMR). This property is useful in designing DNG metamaterial with single type of inclusion only [13–15].

In this paper, effective permittivity and permeability of a medium consisting of an infinite number of ferromagnetic microwires, as discussed in [16], are evaluated with the help of local field and average field inside a unit cell. An artificial medium is formed by the ferromagnetic microwires placed parallel to each other in free space as shown in Fig. 1. According to the effective medium theory, volume of the whole medium is divided into unit cells identical in shape and size. Each unit cell is chosen such

Received 20 February 2017, Accepted 16 April 2017, Scheduled 22 April 2017
* Corresponding author: Tarun Kumar (tkumar@ddn.upes.ac.in).
[1] Department of Electronics Engineering, University of Petroleum & Energy Studies Dehradun, Uttarakhand-248007, India.
[2] Department of Electronics & Communication Engineering, PES University, Bangalore-560085, India.

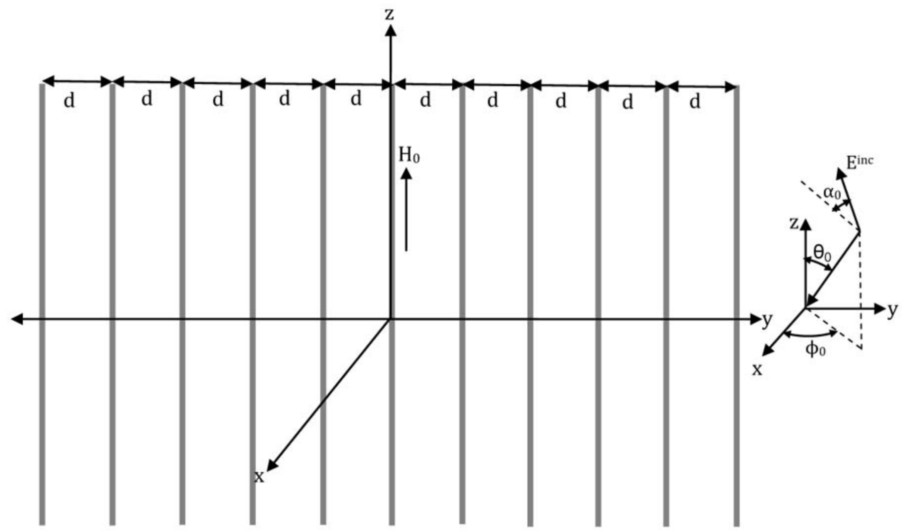

Figure 1. Geometry of the artificial medium formed by ferromagnetic microwires.

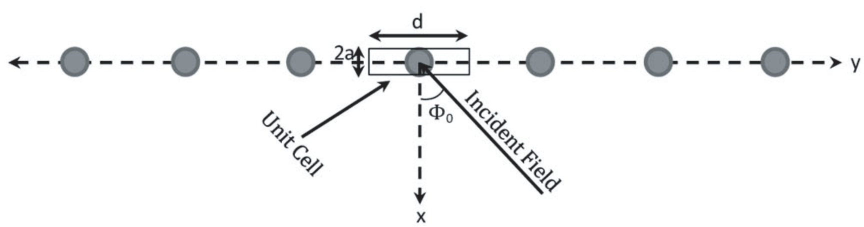

Figure 2. Geometry of the cross section of a unit cell inside the ferromagnetic microwire grid.

that it contains one scatterer [17]. Geometry of such unit cell is shown in Fig. 2. As discussed in [17], the optimum value of the thickness of unit cell is equal to the diameter of the microwires $2a$, while the width and height are kept equal to the spacing among the microwires d. The effective permittivity and permeability of the ferromagnetic microwire grid structure are reported in [17] for the normally incident TM_z polarized uniform plane wave. In [17], effective medium properties are evaluated by assuming the microwires of the grid as made up of impedance loaded perfect electric conductors (PEC) and equivalent sheet current density is calculated. Then, polarization and effective medium properties are obtained by applying homogenization. The approach in [17] is limited for the case of normal incidence and TM_z polarization only. In this paper, a method for the evaluation of effective permittivity and permeability is reported which enables us to evaluate the effective permittivity and permeability of the medium for any arbitrarily polarized uniform plane wave incident obliquely. Scattering from a ferromagnetic microwire grid for the generalized case consisting of an infinite number microwires is discussed in [16]. In this paper, the boundary value type solution for the scattering field coefficients obtained in [16] is directly used to obtain the effective permittivity and permeability of the medium. Numerical results are obtained for TM_z and TE_z polarizations at an angle of incidence $\theta_0 = 45°$, and for polarization angle $\alpha_0 = 45°$ at an angle of incidence $\theta_0 = 45°$. Variation in effective permittivity and effective permeability is shown with respect to the operating frequency in the range of 5–15 GHz. In order to validate the results of the proposed analysis, a comparison is done with the results available in [17] for TM_z polarization at an angle of incidence $\theta_0 = 90°$.

1.1. Local Field and Average Field

In order to gain more insight into the problem, the topic is discussed here as given in [18]. The local field $\mathbf{E}^{loc}$ at the surface of one of the microwire is the sum of the external field $\mathbf{E}^{ext}$ (incident field) and the interaction field created by all the other microwires except the field of the considered reference microwire as discussed in [16]. The local field is defined as [16, 18]:

$$\mathbf{E}^{loc} = \mathbf{E}^{ext} + \sum_{j \neq i}^{+\infty} \mathbf{E}^{ij}. \tag{1}$$

We can define the total field at the surface of reference microwire as

$$\mathbf{E}^{total} = \mathbf{E}^{loc} + \mathbf{E}_i^s \tag{2}$$

Here, $\mathbf{E}_i^s$ is the scattered field of reference microwire located at position number i and $\mathbf{E}^{ij}$ denotes the electric field created by the microwire located at position number j at the surface of the microwire located at position number i. For the case of an infinite and lossless system, the series in Eq. (1) does not converge. More precisely, the result depends on the order of the summation. For finite number of microwires, the result depends on the sample shape and size. Although this problem cannot be completely resolved yet, we can avoid it if we calculate the difference of the local field and the average field, instead of the local field as such. This is consistent with the classical approach used to model materials which are fundamentally based on averaging of the fields. Averaging permits us to skip irrelevant degrees of freedom that describe individual small particle. This method enables us to formulate the macroscopic field equations and the effective medium relations.

Let us consider the artificial material as a collection of unit cells which contains only one particle. These cell are arranged in such a manner that the entire volume of the material is composed of the sum of total volume of unit cells. The spatial average over such a unit cell is defined as

$$\hat{\mathbf{E}} = \frac{1}{V} \int_V \mathbf{E}(\mathbf{r}) dV. \tag{3}$$

The integration is performed over the volume V of a unit cell, and $\mathbf{E}(\mathbf{r})$ is the microscopic electric field. The macroscopic Maxwell equations and the corresponding boundary conditions are formulated for these average fields. It is clear that the local field acting the surface of the microwire is different from the average field because the average field includes the field of all microwires including the reference microwire itself while the local field excludes the field of reference microwire. This difference is given as

$$\mathbf{E}^{loc} - \hat{\mathbf{E}} = \mathbf{E}^{ext} - \hat{\mathbf{E}}^{ext} + \sum_{j \neq i}^{+\infty} \left(\mathbf{E}^{ij} - \hat{\mathbf{E}^{ij}} \right), \tag{4}$$

It is observed in many applications that all sources are located far from any point inside the medium as compared to the size of the unit cell. In such case, the difference between the field at any point in the medium and the average of the field over a unit cell can be neglected provided that the cell size is much less than the wavelength. Thus,

$$\mathbf{E}^{ext} - \hat{\mathbf{E}}^{ext} \approx 0 \tag{5}$$

Now, let us consider the summation in Eq. (4). If the microwire j is at a very large distance from the microwire at i, the difference between the electric field $\mathbf{E}^{ij}$ at the location of i^{th} microwire and the average of the same field $\hat{\mathbf{E}}^{ij}$ over the unit cell of i^{th} microwire is negligible. If the size of all the unit cells is very small in comparison to the wavelength, quasistatic approximation can be used and the field due to distant microwires can be approximated by static field of electric dipoles that decays as $\frac{1}{R^3}$. The difference of the fields given by Eq. (4) decays much faster as $\frac{1}{R^5}$. For an anisotropic periodic lattice, the summation in Eq. (4) converges quickly to a constant. This constant depends upon the geometry of the unit cell and a small term of the order of $(\frac{a}{R_{\max}})^2$, where a is the size of unit cell and $R_{\max}$ is the extent of the sample of composite medium. If microwires are arranged symmetrically, the summation term in Eq. (4) tends to zero under quasistatic condition. In a nutshell, we can say that only a few nearest microwires influence the difference between the average and local field in quasistatic condition. Mathematically, the series in Eq. (4) converges absolutely in contrast to the series in Eq. (1). Hence, for a sample that contains a large number of inclusions, the summation in Eq. (4) can be completely neglected. Therefore,

$$\sum_{j\neq i}^{+\infty}\left(\mathbf{E}^{ij}-\hat{\mathbf{E}^{ij}}\right)\approx 0. \tag{6}$$

Hence, considering the assumption made in Eqs. (5) and (6), Eq. (4) is reduced to

$$\mathbf{E}^{loc}-\hat{\mathbf{E}}\approx 0. \tag{7}$$

which means that the local field at the surface of the reference microwire and average field within the unit cell containing reference microwire acts in a similar manner in quasistatic condition provided that the size of inclusions is much less than the wavelength.

2. FORMULATION OF THE PROBLEM

In the case of anisotropic or nonisotropic materials, constitutive parameters (i.e., ϵ and μ) are functions of the direction of the applied field. For example, when each component of the electric flux density **D** in dielectric materials depends on more than one component of the electric field **E**, such dielectrics are called anisotropic dielectrics. The permittivity and susceptibility for such materials cannot be represented by a single value. Instead, for example, $\bar{\bar{\epsilon}}$ takes the form of a 3×3 tensor, which is known as the permittivity tensor. The electric flux density **D** and electric field intensity **E** are not parallel to each other, and they are related by the permittivity tensor $\bar{\bar{\epsilon}}$ in a form given by [19]

$$\mathbf{D} = \bar{\bar{\epsilon}}.\mathbf{E} \tag{8}$$

$$\begin{bmatrix} D_x \\ Dy \\ D_z \end{bmatrix} = \begin{bmatrix} \epsilon_{xx} & \epsilon_{xy} & \epsilon_{xz} \\ \epsilon_{yx} & \epsilon_{yy} & \epsilon_{yz} \\ \epsilon_{zx} & \epsilon_{zy} & \epsilon_{zz} \end{bmatrix} \begin{bmatrix} E_x \\ Ey \\ E_z \end{bmatrix}, \tag{9}$$

or in terms of components

$$D_x = \epsilon_{xx}E_x + \epsilon_{xy}E_y + \epsilon_{xz}E_z, \tag{10}$$

$$D_y = \epsilon_{yx}E_x + \epsilon_{yy}E_y + \epsilon_{yz}E_z, \tag{11}$$

$$D_z = \epsilon_{zx}E_x + \epsilon_{zy}E_y + \epsilon_{zz}E_z. \tag{12}$$

The permittivity tensor can be written as a 3×3 matrix [19]

$$\bar{\bar{\epsilon}} = \begin{bmatrix} \epsilon_{xx} & \epsilon_{xy} & \epsilon_{xz} \\ \epsilon_{yx} & \epsilon_{yy} & \epsilon_{yz} \\ \epsilon_{zx} & \epsilon_{zy} & \epsilon_{zz} \end{bmatrix}, \tag{13}$$

where each entry in the matrix may be a complex number. All the entries of the permittivity tensor are not necessarily nonzero for anisotropic materials. For some anisotropic materials, only the diagonal elements $(\epsilon_{xx}, \epsilon_{yy}, \epsilon_{zz})$, are nonzero which are referred to as the principal permittivity components [19].

Here, we have assumed that the medium formed by infinite number of ferromagnetic microwires possesses only the diagonal elements $(\epsilon_{xx}, \epsilon_{yy}, \epsilon_{zz})$ in the permittivity matrix used in our analysis. Hence, Eqs. (10)–(12) reduces to

$$D_x = \epsilon_{xx}E_x, \tag{14}$$

$$D_y = \epsilon_{yy}E_y, \tag{15}$$

$$D_z = \epsilon_{zz}E_z. \tag{16}$$

Similarly, for the permeability matrix

$$B_x = \mu_{xx}H_x, \tag{17}$$

$$B_y = \mu_{yy}H_y, \tag{18}$$

$$B_z = \mu_{zz}H_z. \tag{19}$$

Now, the effective permittivity and permeability are defined as [20–22]:

$$\epsilon_0\epsilon^{eff} = \frac{\langle \mathbf{D} \rangle_V}{\langle \mathbf{E} \rangle_V}, \tag{20}$$

and

$$\mu_0\mu^{eff} = \frac{\langle \mathbf{B} \rangle_V}{\langle \mathbf{H} \rangle_V}, \tag{21}$$

where $\langle \mathbf{D} \rangle_V, \langle \mathbf{B} \rangle_V, \langle \mathbf{E} \rangle_V$ and $\langle \mathbf{H} \rangle_V$ are the average values of the electric displacement, magnetic flux density and electric and magnetic field intensity over the volume of a unit cell, respectively. In the previous section, we have shown that the difference between the local field and average field is n eligible under quasi-static condition. Hence, we will assume $\langle \mathbf{E} \rangle_V \simeq \mathbf{E}^{loc}$ in our analysis.

For the diluted plasma, the average value of electric displacement $\langle \mathbf{D}_V \rangle$ is obtained as [21, 22]:

$$\langle \mathbf{D} \rangle_V = \epsilon_0 \mathbf{E}^{loc} + f \langle \mathbf{D} \rangle_{wire}, \tag{22}$$

where $f = (\pi a^2/td)$ is called the filling factor [21]. Here, a is the radius of microwire, t the thickness of the microwire grid, d the microwire spacing and $\langle \mathbf{D} \rangle_{wire}$ the electric displacement averaged over the wire. As discussed in the previous section, the difference between local field and average field within a unit cell is negligible under quasistatic condition. As discussed in [16], the microwires of infinite length, each with radius a and having applied internal axial magnetization H_0 are placed parallel to one another in y-z plane with the uniform spacing d as shown in Fig. 1. The reference microwire is assumed to be placed along the z-axis and impinged upon by uniform plane wave with polarization angle α_0 and incident angle θ_0. From Maxwell's equations,

$$\nabla \times \mathbf{H} = j\omega \mathbf{D} \tag{23}$$

$$\Rightarrow \qquad \mathbf{D} = \frac{1}{j\omega}\left(\nabla \times \mathbf{H}\right), \tag{24}$$

and

$$\nabla \times \mathbf{E} = -j\omega \mathbf{B} \tag{25}$$

$$\Rightarrow \qquad \mathbf{B} = -\frac{1}{j\omega}\left(\nabla \times \mathbf{E}\right). \tag{26}$$

In cylindrical coordinates

$$\mathbf{D} = \frac{1}{j\omega\rho}\begin{bmatrix} \hat{a_\rho} & \rho\hat{a_\phi} & \hat{a_z} \\ \dfrac{\partial}{\partial\rho} & \dfrac{\partial}{\partial\phi} & \dfrac{\partial}{\partial z} \\ H_\rho & \rho H_\phi & H_z \end{bmatrix}, \tag{27}$$

The z-component of $\mathbf{D}$ can be obtained with the help of (27) as

$$D_z = \frac{1}{j\omega\rho}\left[\frac{\partial}{\partial\rho}\rho H_\phi - \frac{\partial}{\partial\phi}H_\rho\right] \tag{28}$$

As the radius of microwire is considered to be much smaller than wavelength, we assume that the scattered field is independent of azimuthal coordinate ϕ. Hence, substituting $\frac{\partial}{\partial\phi} = 0$ in Eq. (28), we get

$$D_z = \frac{1}{j\omega\rho}\left[\rho\frac{\partial}{\partial\rho}H_\phi + H_\phi\right] \tag{29}$$

As the continuity of the tangential fields at the surface of microwire is already verified in [16], field components just inside the microwire are equal to the total field just outside the microwire. Hence, we can calculate the total electric flux density at the surface of the microwire, D_z^{wire} with the help of Eq. (29) by substituting H_ϕ^{total} for H_ϕ in Eq. (29), which is given as

$$H_\phi^{total} = H_{\phi_0}^{loc} + H_{\phi_0}^{s} \tag{30}$$

where $H_{\phi_0}^{total}$ is the ϕ component of the total magnetic field, and $H_{\phi_0}^{loc}$ is the ϕ component of the local magnetic field at the surface of the reference microwire as discussed in [16]. The local field components can be calculated by adding the incident field to the scattered field from the other microwires at the surface of the reference microwires. For example, The $H_{\phi_0}^{loc}$ components can be represented as

$$H_{\phi_0}^{loc} = H_{\phi_0}^{inc} + \sum_{l=-\infty}^{+\infty} H_{\phi_l}^{s}; \quad l \neq 0. \tag{31}$$

H_{ϕ}^{total} can be calculated after substituting the values of $H_{\phi_0}^{inc}$, $H_{\phi_0}^{s}$ and $H_{\phi_0}^{loc}$ as given in [16] into Eqs. (30) and (31):

$$H_{\phi}^{total} = \frac{j}{\eta_0}\left[\cos\alpha_0\left\{J_1\left(\beta_{\rho 0}\rho\right) + C_0 H_1^{(2)}\left(\beta_{\rho 0}\rho\right)\right\} + C_0 J_1\left(\beta_{\rho 0\rho}\right) H_0^{(2)}\left(\beta_{\rho 0} d_{ig}\right)\right]. \tag{32}$$

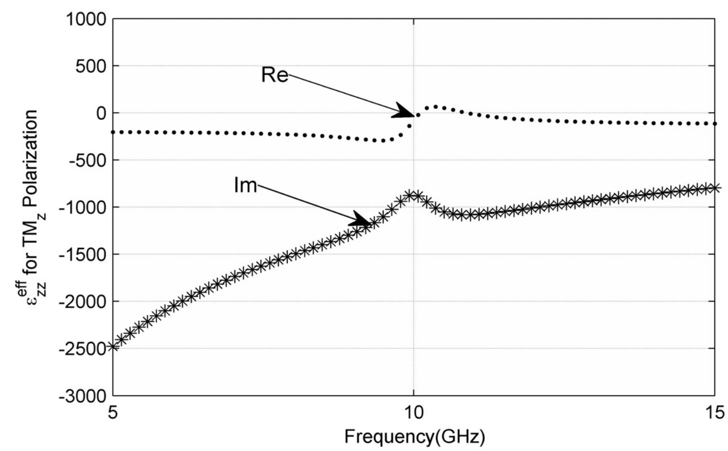

(a)

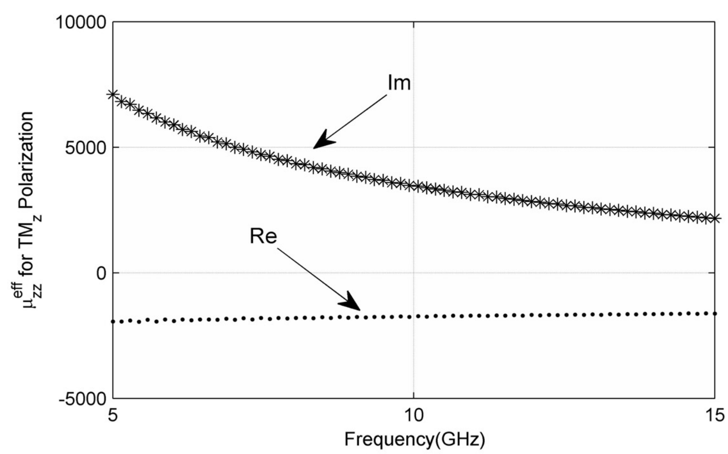

(b)

Figure 3. Real and imaginary parts of the (a) ϵ_{zz} component of the Effective permittivity (b) μ_{zz} component of the Effective permeability for a grid of ferromagnetic microwires of 1 μm radius and 3 mm separation between wires for TM_z Polarization.

Finally, D_z^{wire} is found with the help (29) to be

$$D_z^{wire} = -\frac{1}{\omega\eta_0}\left[\left(\cos\alpha_0 + C_0 H_0^{(2)}\left(\beta_{\rho 0} dig\right)\right)\left(\beta_{\rho 0}\rho J_2\left(\beta_{\rho 0}\rho\right) - \frac{2}{\rho} J_1\left(\beta_{\rho 0}\rho\right)\right)\right. \quad (33)$$

$$\left. + C_0\left(\beta_{\rho 0}\rho H_2^{(2)}\left(\beta_{\rho 0}\rho\right) - \frac{2}{\rho} H_1^{(2)}\left(\beta_{\rho 0}\rho\right)\right)\right]. \quad (34)$$

Now, the z-component of the local electric field, E_z^{loc}, is given by

$$E_{z_0}^{loc} = E_{z_0}^{inc} + \sum_{l=-\infty}^{+\infty} E_{z_l}^{s}; \quad l \neq 0. \quad (35)$$

Finally, ϵ_{zz}^{eff}, $\epsilon_{\rho\rho}^{eff}$ and $\epsilon_{\phi\phi}^{eff}$ can be obtained with the help of Eqs. (14), (15) and (16) as

$$\epsilon_0 \epsilon_{zz}^{eff} = \frac{\langle D_z \rangle_V}{E_z^{loc}}. \quad (36)$$

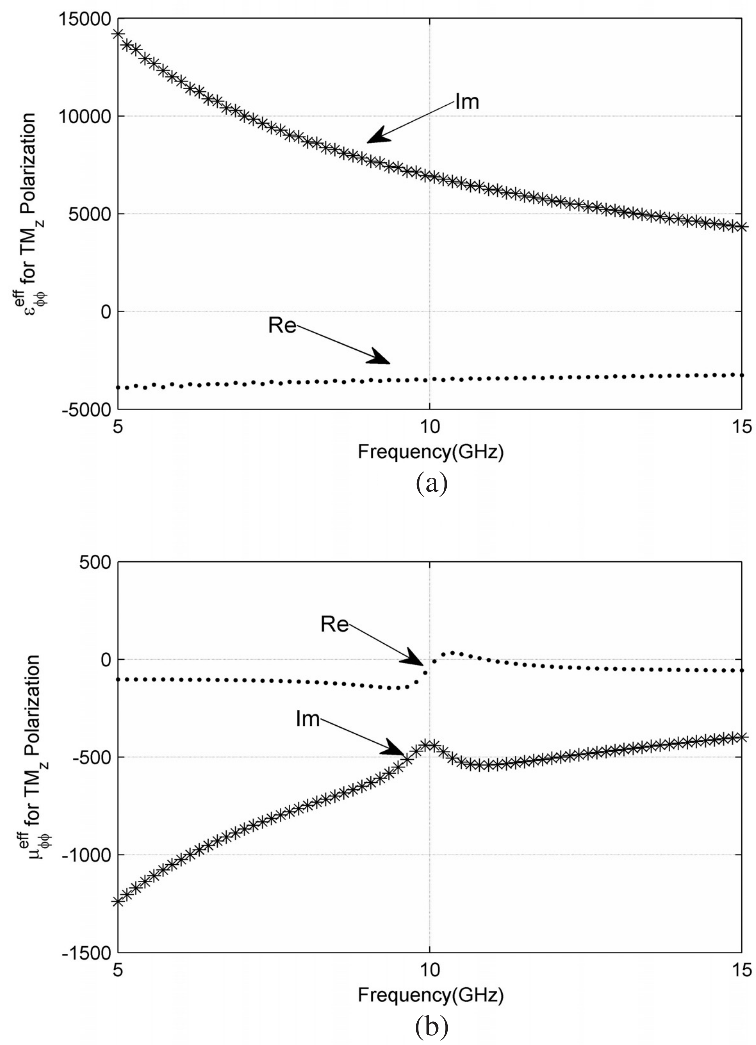

Figure 4. Real and imaginary parts of the (a) $\epsilon_{\phi\phi}$ component of the Effective permittivity (b) $\mu_{\phi\phi}$ component of the Effective permeability for a grid of ferromagnetic microwires of 1 µm radius and 3 mm separation between wires for TM_z Polarization.

$$\epsilon_0 \epsilon_{\rho\rho}^{eff} = \frac{\langle D_\rho \rangle_V}{E_\rho^{loc}}, \tag{37}$$

and

$$\epsilon_0 \epsilon_{\phi\phi}^{eff} = \frac{\langle D_\phi \rangle_V}{E_\phi^{loc}}. \tag{38}$$

Similarly, effective permeability can be obtained by starting from Eq. (26) as

$$B_z = \frac{-1}{j\omega\rho} \left[\frac{d}{d\rho} (\rho E_\phi) - \frac{dE_\rho}{d\phi} \right] \tag{39}$$

Once again, as the radius of microwire is considered to be much smaller than wavelength, we assume that the scattered field is independent of azimuthal coordinate ϕ. Hence, substituting for $\frac{\partial}{\partial \phi} = 0$ in Eq. (39), we get

$$B_z = \frac{-1}{j\omega\rho} \left[\rho \frac{\partial}{\partial \rho} E_\phi + E_\phi \right] \tag{40}$$

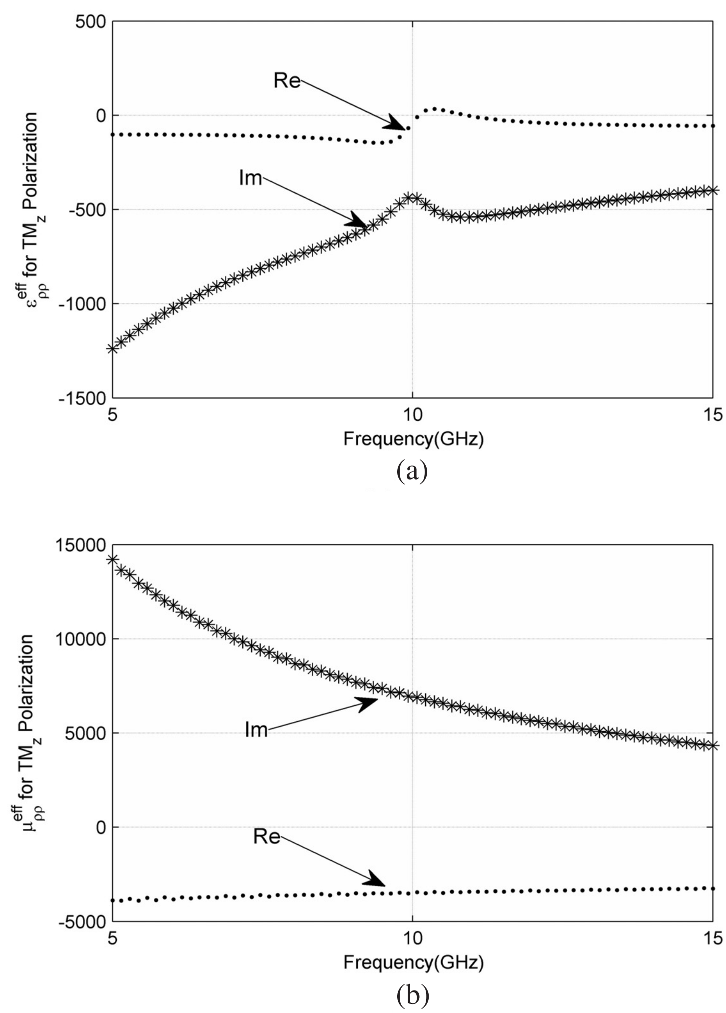

Figure 5. Real and imaginary parts of the (a) $\epsilon_{\rho\rho}$ component of the Effective permittivity (b) $\mu_{\rho\rho}$ component of the Effective permeability for a grid of ferromagnetic microwires of 1 μm radius and 3 mm separation between wires for TM_z Polarization.

Now, we have to calculate the total electric flux density B_z^{total} with the help of Eq. (41) by substituting E_ϕ^{total} which is given as

$$E_\phi^{total} = E_{\phi_0}^s + E_{\phi_0}^{loc}; \tag{41}$$

where $E_{\phi_0}^{loc}$ is the local field components at the surface of the reference microwire. The local field components can be calculated by adding the incident field to the scattered field from the other microwires at the surface of the reference microwires. For example, the $E_{\phi_0}^{loc}$ components can be represented as

$$E_{\phi_0}^{loc} = E_{\phi_0}^{inc} + \sum_{l=-\infty}^{+\infty} E_{\phi_l}^s; \quad l \neq 0. \tag{42}$$

E_ϕ^{total} can be calculated after substituting the values of $E_{\phi_0}^{inc}$, $E_{\phi_0}^s$ and $E_{\phi_0}^{loc}$ as given in [16] into Eqs. (41) and (42) to be

$$E_\phi^{total} = -j\left[\sin\alpha_0 J_1\left(\beta_{\rho 0}\rho\right) + D_0 H_1^{(2)}\left(\beta_{\rho 0}\rho\right) + D_0 J_1\left(\beta_{\rho 0 \rho}\right) H_0^{(2)}\left(\beta_{\rho 0} d_{ig}\right)\right] \tag{43}$$

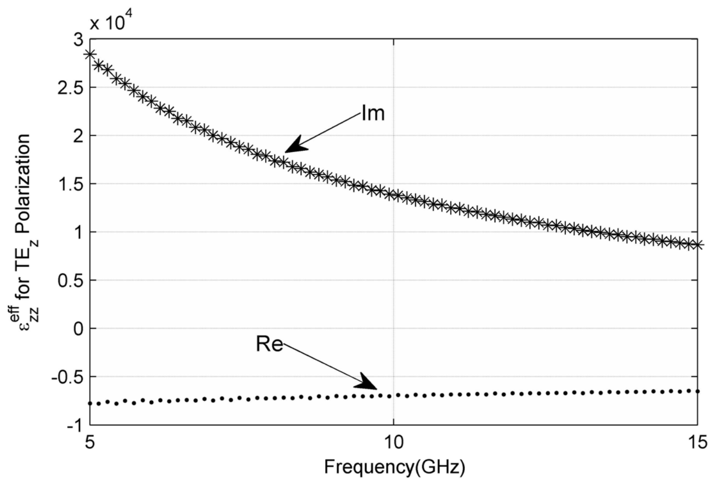

(a)

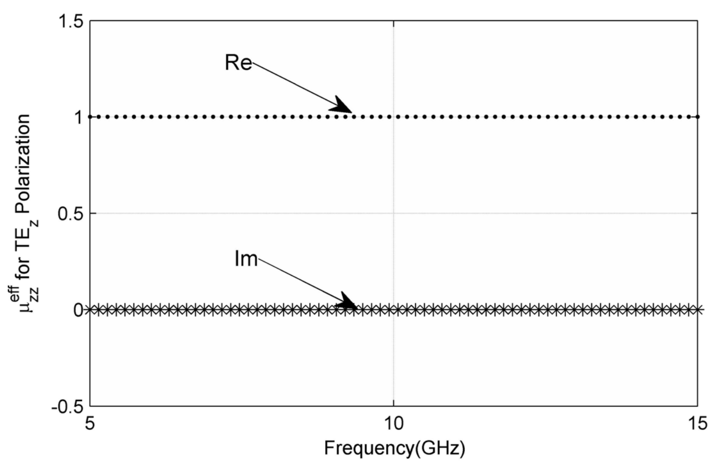

(b)

Figure 6. Real and imaginary parts of the (a) ϵ_{zz} component of the Effective permittivity (b) μ_{zz} component of the Effective permeability for a grid of ferromagnetic microwires of 1 μm radius and 3 mm separation between wires for TE_z Polarization.

Now, B_z^{wire} is found with the help of Eq. (40) to be

$$B_z^{wire} = -\frac{1}{\omega}\left[\left(\sin\alpha_0 + D_0 H_0^{(2)}\left(\beta_{\rho 0} d_{ig}\right)\right)\left(\beta_{\rho 0}\rho J_2\left(\beta_{\rho 0}\rho\right) - \frac{2}{\rho}J_1\left(\beta_{\rho 0}\rho\right)\right)\right. \tag{44}$$

$$\left. + jD_0\left(\beta_{\rho 0}\rho H_2^{(2)}\left(\beta_{\rho 0}\rho\right) - \frac{2}{\rho}H_1^{(2)}\left(\beta_{\rho 0}\rho\right)\right)\right] \tag{45}$$

The z-component of the local magnetic field, H_{z0}^{loc}, is expressed as in [16]

$$H_{z_0}^{loc} = H_{z_0}^{inc} + \sum_{l=-\infty}^{+\infty} H_{z_l}^{s}; \quad l \neq 0. \tag{46}$$

Now, the average magnetic flux density $\langle \mathbf{B} \rangle_V$ over the volume of periodic cell is defined as [21, 22]:

$$\langle \mathbf{B} \rangle_V = \mu_0 \mathbf{H}^{loc} + f \langle \mathbf{B} \rangle_{wire}. \tag{47}$$

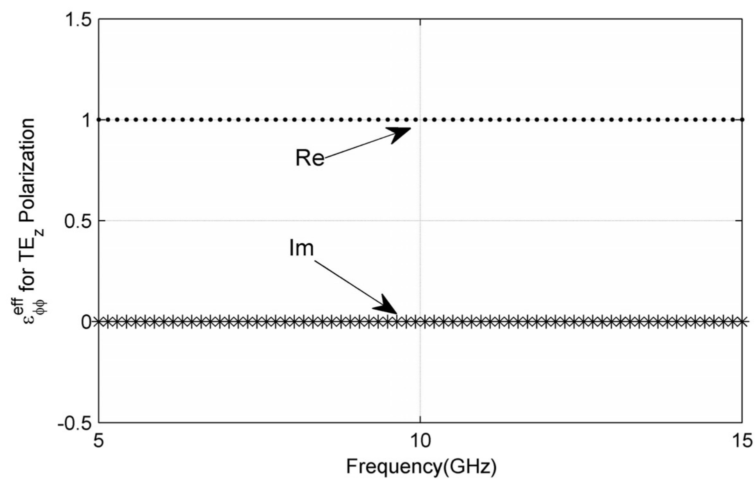

(a)

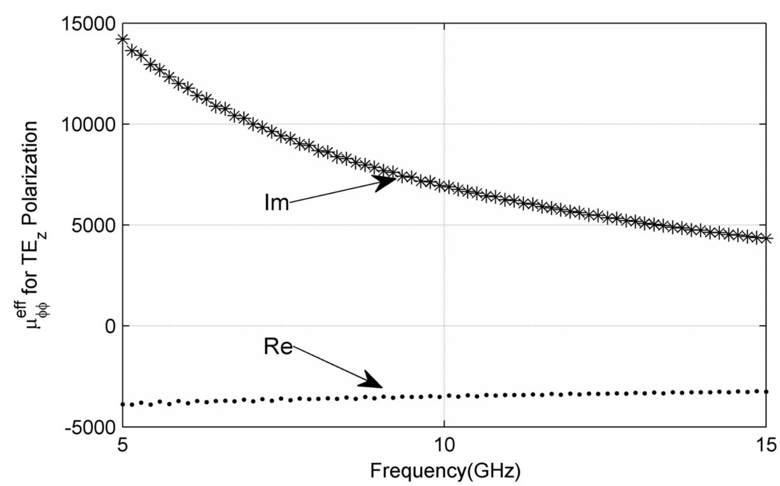

(b)

Figure 7. Real and imaginary parts of the (a) $\epsilon_{\phi\phi}$ component of the Effective permittivity (b) $\mu_{\phi\phi}$ component of the Effective permeability for a grid of ferromagnetic microwires of 1 µm radius and 3 mm separation between wires for TE_z polarization.

Finally, μ_{zz}^{eff}, $\mu_{\rho\rho}^{eff}$ and $\mu_{\phi\phi}^{eff}$ can be obtained with the help of Eqs. (17), (18) and (19) to be

$$\mu_0 \mu_{zz}^{eff} = \frac{\langle B_z \rangle_V}{H_z^{loc}} \tag{48}$$

$$\mu_0 \mu_{\rho\rho}^{eff} = \frac{\langle B_\rho \rangle_V}{H_\rho^{loc}} \tag{49}$$

$$\mu_0 \mu_{\phi\phi}^{eff} = \frac{\langle B_\phi \rangle_V}{H_\phi^{loc}} \tag{50}$$

3. NUMERICAL RESULTS

In this section, numerical results for the diagonal components of the effective permittivity and permeability are obtained for a Cobalt based ferrite microwire grid (see Fig. 1) with the following specifications [16, 17]: radius $a = 1\,\mu\text{m}$, conductivity $\sigma = 6.7 \times 10^5\,\text{S/m}$, gyromagnetic ratio $\gamma = 2 \times 10^{11}\,\text{T}^{-1}\,\text{s}^{-1}$, saturation magnetization $\mu_0 M_s = 0.55\,\text{T}$, magnetic loss factor $\delta = 0.02$, internal

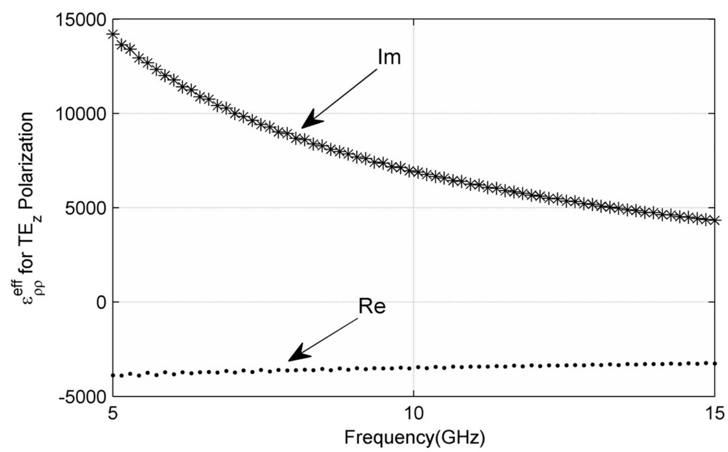

(a)

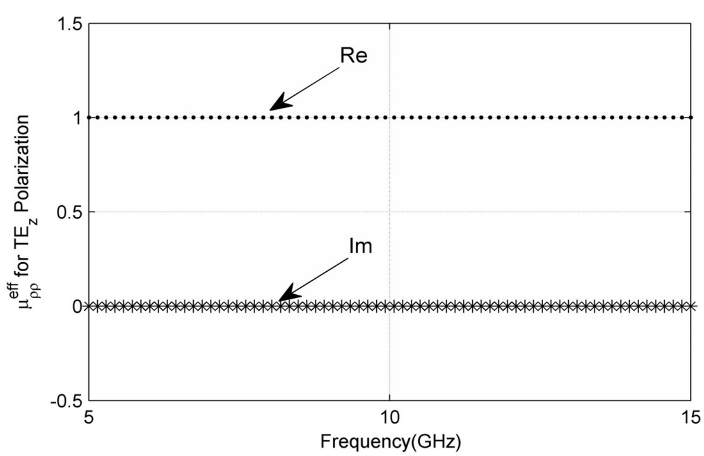

(b)

Figure 8. Real and imaginary parts of the (a) $\epsilon_{\rho\rho}$ component of the Effective permittivity (b) $\mu_{\rho\rho}$ component of the Effective permeability for a grid of ferromagnetic microwires of 1 μm radius and 3 mm separation between wires for TE_z polarization.

magnetization $H_0 = 113.45\,\mathrm{kA/m}$ along the z-coordinate and an operating frequency band of 5–15 GHz is assumed. Numerical results are obtained for TM_z and TE_z polarizations (i.e., $\alpha_0 = 0°$ and $90°$) at an angle of incidence $\theta_0 = 45°$, and for polarization angle $\alpha_0 = 45°$ at an angle of incidence $\theta_0 = 45°$. Variation in effective permittivity and effective permeability is shown with respect to the operating frequency in the range of 5–15 GHz. A comparison of the numerical results obtained for TM_z and normal incidence is also made with the results given in [17].

3.1. TM_z Polarization

Figures 3, 4 and 5 show the numerical results for $\epsilon_{zz} - \mu_{zz}$, $\epsilon_{\phi\phi} - \mu_{\phi\phi}$ and $\epsilon_{\rho\rho} - \mu_{\rho\rho}$ components of the effective permittivity and permeability for TM_z polarization, respectively. It can be seen that the real parts of all the three diagonal components of effective permittivity and permeability are negative in the entire range of the frequency 5–15 GHz which results in strong reflection. Further, $\mu_{zz}, \epsilon_{\phi\phi}$ and $\mu_{\rho\rho}$ remain unaffected by the effect of FMR while $\epsilon_{zz}, \epsilon_{\rho\rho}$ and $\mu_{\phi\phi}$ depict the effect of FMR. Effect of FMR on ϵ_{zz} and $\epsilon_{\rho\rho}$ verifies that the dielectric properties of the medium are governed by the magnetic

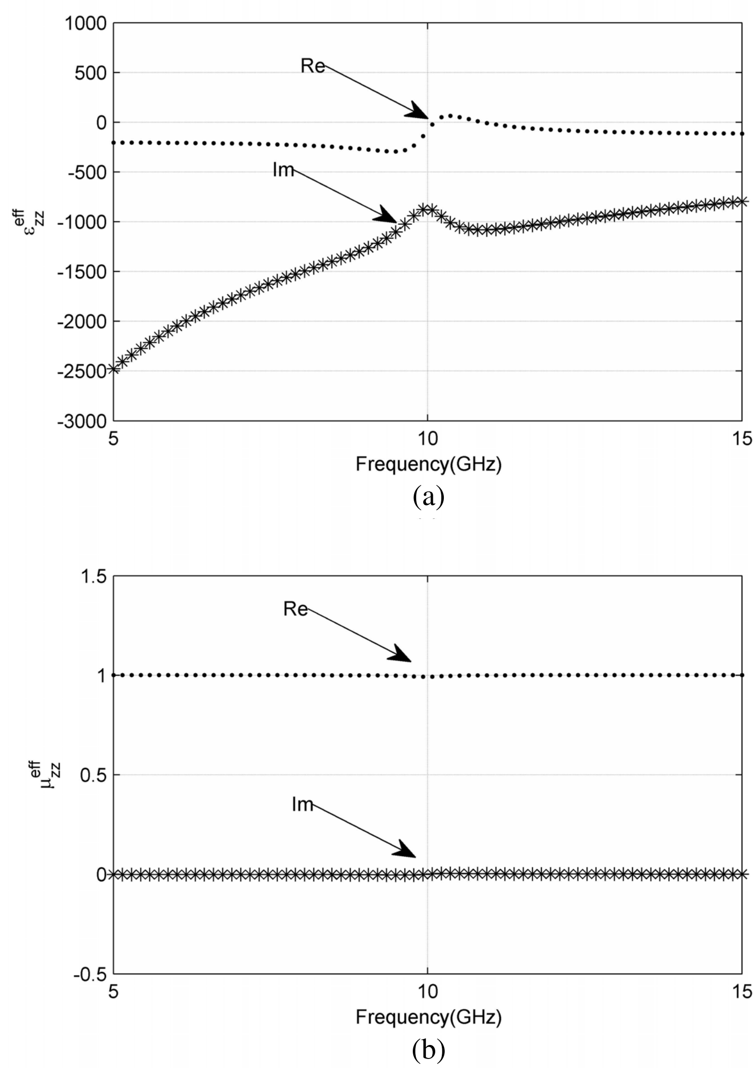

Figure 9. Real and imaginary parts of the (a) ϵ_{zz} component of the Effective permittivity (b) μ_{zz} component of the Effective permeability for a grid of ferromagnetic microwires of 1 µm radius and 3 mm separation between wires for $\alpha_0 = 45°$ and $\theta_0 = 45°$.

response of the medium. The imaginary part of $\mu_{zz}, \epsilon_{\phi\phi}$ and $\mu_{\rho\rho}$ is positive with a large value which represents huge losses inside the medium. Moreover, it can be seen that Fig. 6(a) and Fig. 6(b) have similar kind of plots for $\epsilon_{\phi\phi}$ and $\mu_{\rho\rho}$, respectively which suggests mutual coupling among the effective medium properties.

3.2. TE_z Polarization

Figures 6, 7 and 8 show the numerical results for $\epsilon_{zz} - \mu_{zz}$, $\epsilon_{\phi\phi} - \mu_{\phi\phi}$ and $\epsilon_{\rho\rho} - \mu_{\rho\rho}$ components of the effective permittivity and permeability for TE_z polarization, respectively. It can be seen that none of the three diagonal components of effective permittivity and permeability have negative real part simultaneously. The real part of $\epsilon_{zz}, \mu_{\phi\phi}$ and $\epsilon_{\rho\rho}$ are negative in the entire range of the frequency 5–15 GHz. While $\mathrm{Re}[\mu_{zz}], \mathrm{Re}[\epsilon_{\phi\phi}]$ and $\mathrm{Re}[\mu_{\rho\rho}]$ remain equal to 1 and $\mathrm{Im}[\mu_{zz}], \mathrm{Im}[\epsilon_{\phi\phi}]$ and $\mathrm{Im}[\mu_{\rho\rho}]$ remain equal to 0 (i.e., equal to the free space permittivity and permeability) which results in weak scattering. Moreover, all components remain unaffected by the effect of FMR as there is no FMR inside the ferrite medium in case of TE_z Polarization. It may be seen in Fig. 4(b), Fig. 7 and Fig. 8 that the effective permittivity and effective permeability of the medium are mutually coupled.

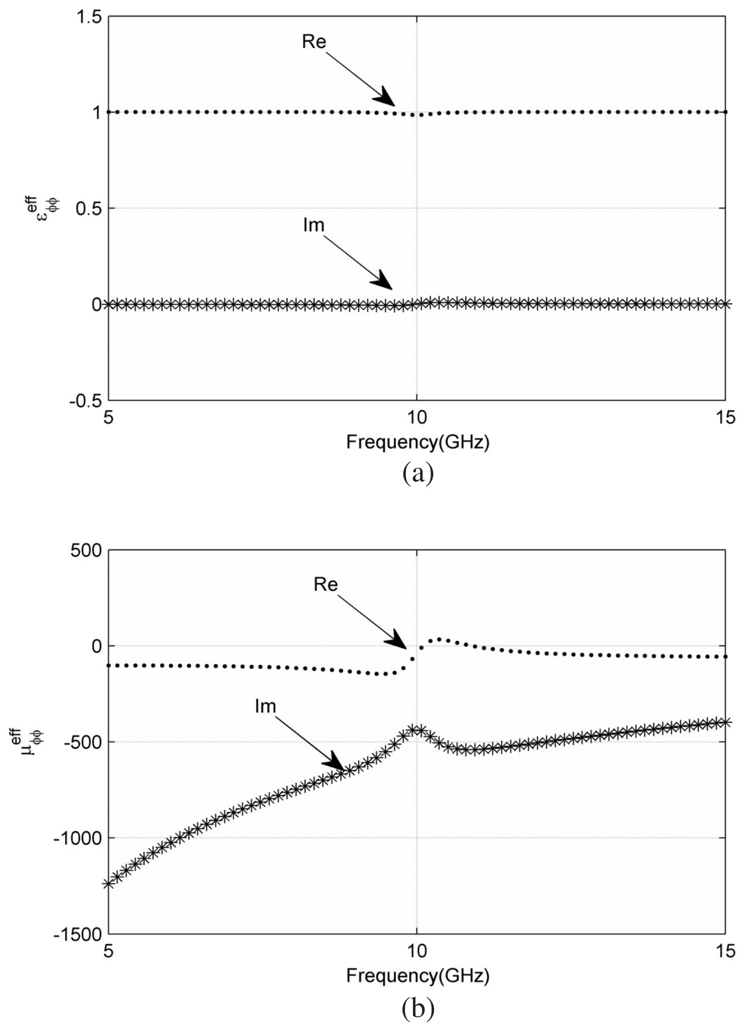

Figure 10. Real and imaginary parts of the (a) $\epsilon_{\phi\phi}$ component of the Effective permittivity (b) $\mu_{\phi\phi}$ component of the Effective permeability for a grid of ferromagnetic microwires of 1 μm radius and 3 mm separation between wires for $\alpha_0 = 45°$ and $\theta_0 = 45°$.

3.3. Arbitrary Polarization and Incident Angle

Figures 9, 10 and 11 show the numerical results for $\epsilon_{zz} - \mu_{zz}$, $\epsilon_{\phi\phi} - \mu_{\phi\phi}$ and $\epsilon_{\rho\rho} - \mu_{\rho\rho}$ components of the effective permittivity and effective permeability for polarization angle, $\alpha_0 = 45^\circ$ and incident angle, $\theta_0 = 45^\circ$, respectively. Once again, it can be seen that none of the three diagonal components of effective permittivity and permeability have negative real parts simultaneously. However, the real and imaginary parts of $\epsilon_{zz}, \epsilon_{\rho\rho}$ and $\mu_{\phi\phi}$ components of effective permittivity and effective permeability are negative in the entire range of the frequency 5–15 GHz. These plots are also similar to the case of TM_z polarization with only slightly changed magnitudes. Once again, the real parts of $\mu_{zz}, \epsilon_{\phi\phi}$ and $\mu_{\rho\rho}$ components of the effective permittivity and effective permeability remain equal to 1 with imaginary parts equal to zero (i.e., the free space permittivity and permeability). Further, all the plots depict the effect of FMR due to the co-polarization component in this case.

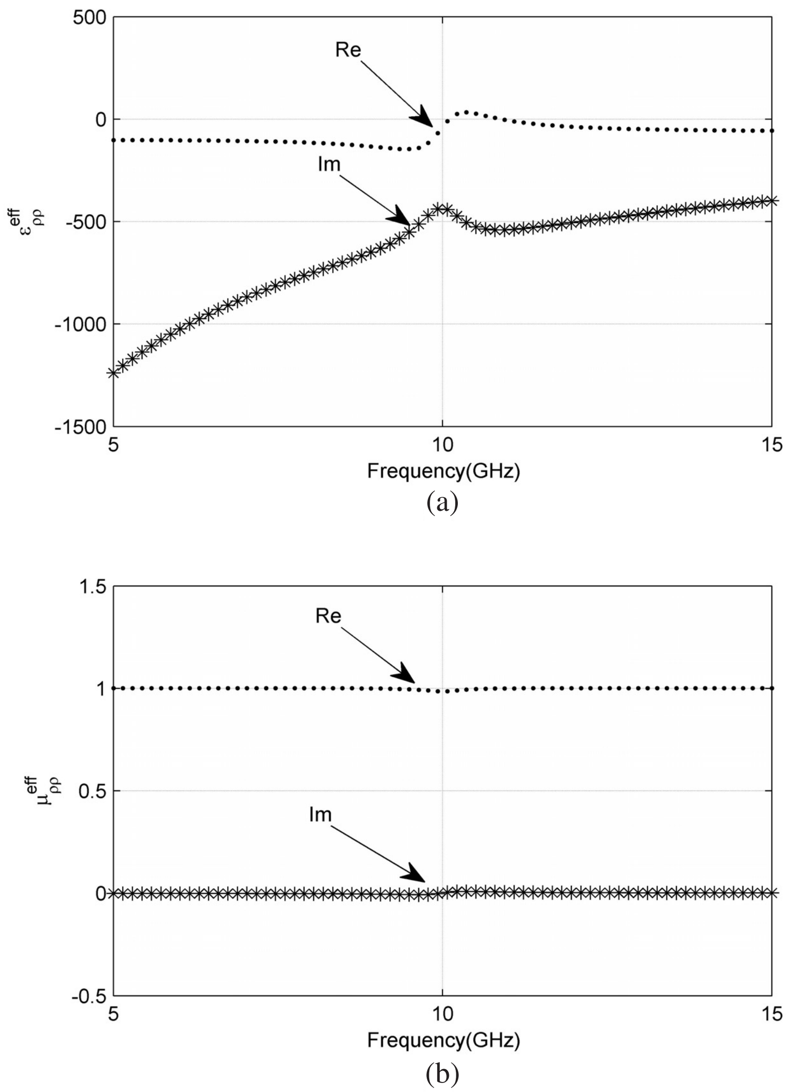

Figure 11. Real and imaginary parts of the (a) $\epsilon_{\rho\rho}$ component of the Effective permittivity (b) $\mu_{\rho\rho}$ component of the Effective permeability for a grid of ferromagnetic microwires of 1 µm radius and 3 mm separation between wires for $\alpha_0 = 45^\circ$ and $\theta_0 = 45^\circ$.

4. COMPARISON OF THE RESULTS

Figures 12(a) and 12(b) show the comparison of the numerical results of the proposed analysis with the results of effective permittivity given in [17] for TM_z polarization and normal incidence case at applied magnetization of 113.45 kA/m. Comparison of the results verifies the negative values of the real and imaginary parts of the effective permittivity obtained through the proposed analysis. Although the two results are not matched quantitatively, the effect of FMR and characteristics of the plots are matched qualitatively. This mismatch arises due to the assumption made in [17] by Liberal et al. which states that the medium is considered to be an equivalent current sheet. There is no such assumption made in the proposed analysis as it is based upon the tangential boundary conditions.

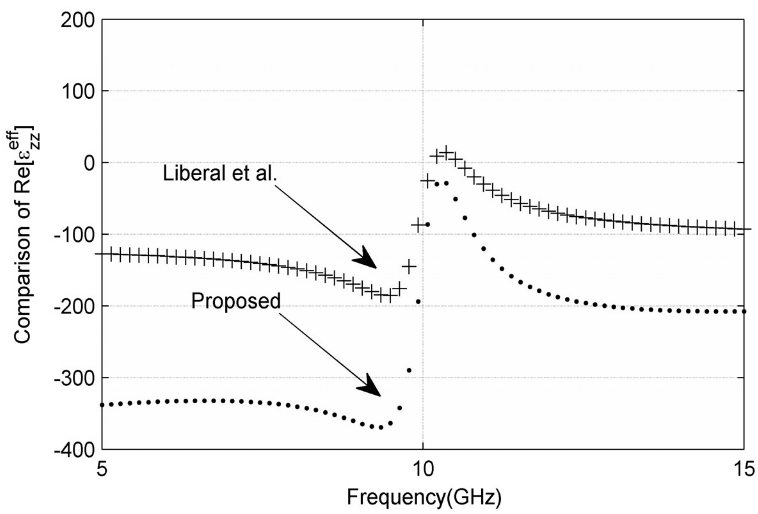

(a)

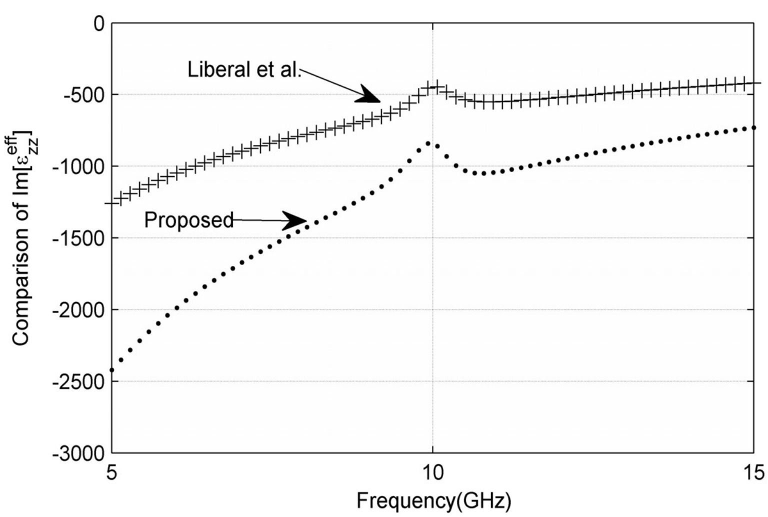

(b)

Figure 12. (a) Comparison of the Real parts of Effective permittivity. (b) Comparison of the imaginary parts of Effective permittivity with the results given in [17] by Liberal et al., for the considered ferromagnetic microwire grid for TM_z polarization.

5. CONCLUSION

The work discussed in this paper pertains to the theoretical analysis of the diagonal components of tensor effective permittivity and permeability of a medium formed by a planar grid consisting of ferromagnetic microwires. The analysis is carried out with the help of local and average field components within a unit cell. The method available in the literature evaluates the effective permittivity by assuming the microwire grid as an impedance loaded surface and then calculates the equivalent current density. That approach is capable of evaluating the effective permittivity only for TM_z polarization and normal incidence case. On the other hand, the method discussed in this paper has analyzed effective permittivity and permeability for an arbitrary polarization and oblique incidence. Numerical results are obtained for the principal diagonal components of the tensor effective permittivity and permeability for TM_z, TE_z and arbitrary polarizations at an angle of incidence $\theta_0 = 45^\circ$ through MATLAB. Numerical results have shown that the medium formed by a ferromagnetic microwire grid behaves as a DNG medium for a frequency band of 5–10 GHz only for TM_z polarization. For other polarizations, the real part of effective permittivity and permeability are not negative simultaneously. However they are found to be negative individually. Numerical results of the proposed analysis, specialized to the case of normal incidence and TM_z, are compared with the results available in the literature. The results obtained in this paper have shown remarkable similarity with the results available in the literature and are thus validated.

REFERENCES

1. Lindell, I. V., A. H. Sihvola, J. Kurkijarvi, and K. F. Lindman, "The last Hertzian, and a harbinger of electromagnetic chirality," *IEEE Antennas Propag. Mag.*, Vol. 34, No. 3, 24–30, 1992.
2. Pendry, J. B., A. Holden, W. Stewart, and I. Youngs, "Extremely low frequency plasmons in metallic mesostructures," *Phys. Rev. Lett.*, Vol. 76, No. 25, 4773–4776, 1996.
3. Smith, D. R., W. J. Padilla, N. S. C. Nemat, and S. Schultz, "Composite medium with simultaneously negative permeability and permittivity," *Phys. Rev. Lett.*, Vol. 84, 4184–4187, 2000.
4. Shelby, R. A., D. R. Smith, and S. Schultz, "Experimental verification of a negative index of refraction," *Science*, Vol. 292, 77–79, 2001.
5. Walser, R. M., "Electromagnetic metamaterials," *Proc. SPIE*, Vol. 4467, 1–15, July 9, 2001.
6. Pendry, J. B., D. Schurig, and D. R. Smith, "Controlling electromagnetic fields," *Science*, Vol. 312, 1780–1782, 2006.
7. Bose, J. C., "On the rotation of plane of polarization of electric waves by a twisted structure," *Proc. R. Soc. Lond.*, Vol. 63, 146–152, January 1, 1898.
8. Kock, W., "Metallic delay lenses," *Bell System, Technical J.*, Vol. 27, 58–82, 1948.
9. Veselago, V. G., "The electrodynamics of substances with simultaneously negative values of ϵ and μ," *Sov. Phys. Uspekhi*, Vol. 10, No. 4, 509–514, 1968.
10. Pendry, J. B., A. J. Holden, D. J. Robbins, and W. J. Stewart, "Magnetism from conductors and enhanced non-linear phenomena," *IEEE Trans. on Microwave Theory Techn.*, Vol. 47, 2075–2084, 1999.
11. Belov, P., S. Tretyakov, and A. Viitanen, "Dispersion and reflection properties of artificial media formed by regular lattices of ideally conducting wires," *Journal of Electromagnetic Waves and Applications*, Vol. 16, No. 8, 1153–1170, 2002.
12. Christodoulou, C., and J. Kauffman, "On the electromagnetic scattering from infinite rectangular grids with finite conductivity," *IEEE Transactions on Antennas and Propagation*, Vol. 34, No. 2, 144–154, 1986.
13. He, Y., P. He, V. G. Harris, and V. Carmine, "Role of Ferrites in negative index metamaterials," *IEEE Trans. on Magnetics*, Vol. 42, No. 10, 2852–2854, 2006.
14. Carbonell, J., M. H. García, and D. J. Sánchez, "Double negative metamaterials based on ferromagnetic microwires," *Physical Review B*, Vol. 81, 024401-1–024401-6, 2010.

15. Carignan, L., A. Yelon, and D. Ménard, "Ferromagnetic nanowire metamaterials: Theory and applications," *IEEE Trans. Microwave Theory Techn.*, Vol. 59, No. 10, 2568–2586, 2011.
16. Kumar, T., N. Kalyanasundaram, and B. K. Lande, "Analysis of the generalized case of scattering from a ferromagnetic microwire grid," *Progress In Electromagnetics Research M*, Vol. 35, 1–10, 2014.
17. Liberal, I., I. S. Nefedov, I. Ederra, R. Gonzalo, and S. A. Tretyakov, "Electromagnetic response and homogenization of grids of ferromagnetic microwires," *J. Appl. Phys.*, Vol. 110, 064909-1–064909-8, 2011.
18. Tretyakov, S., *Analytical Modeling in Applied Electromagnetics*, 69–81, Artech House, Boston, 2003.
19. Balanis, C. A., *Advanced Engineering Electromagnetics*, 2nd Edition, Chap. 11, 57–606, John Wiley and Sons, 2012.
20. Wilfried, S. and W. Martin, *Semiconductor Optics and Transport Phenomena*, 32–33, Springer-Verlag, Berlin-Heidelberg, 2002.
21. Reynet, O., A. L. Adenot, S. Deprot, and O. Acher, "Effect of the magnetic properties of the inclusions on the high-frequency dielectric response of diluted composites," *Phy. Rev. B*, Vol. 66, 094412-1–094412-9, 2002.
22. Acher, O., M. Ledieu, A. L. Adenot, and O. Reynet, "Microwave properties of diluted composites made of magnetic wires with giant magneto-impedance effect," *IEEE Trans. on Mag.*, Vol. 39, No. 5, 3085–3090, 2003.